Laser-induced damage thresholds of bulk and coating optical materials at 1030 nm, 500 fs

Laurent Gallais* and Mireille Commandré

Aix Marseille Université, CNRS, Centrale Marseille, Institut Fresnel, UMR 7249, 13013 Marseille, France

*Corresponding author: laurent.gallais@fresnel.fr

Received 6 September 2013; revised 24 October 2013; accepted 28 October 2013;
posted 29 October 2013 (Doc. ID 197167); published 18 December 2013

We report on extensive femtosecond laser damage threshold measurements of optical materials in both bulk and thin-film form. This study, which is based on published and new data, involved simple oxide and fluoride films, composite films made from a mixture of two dielectric materials, metallic films, and the surfaces of various bulk materials: oxides, fluorides, semiconductors, and ionic crystals. The samples were tested in comparable conditions at 1030 nm, 375 to 600 fs, under single-pulse irradiation. A large number of different samples prepared by different deposition techniques have been tested, involving classical materials used in the fabrication of optical thin film components (Ag, AlF_3, Al_2O_3, HfO_2, MgF_2, Nb_2O_5, Pt, Sc_2O_3, SiO_2, Ta_2O_5, Y_2O_3, and ZrO_2) and their combination with codeposition processes. Their behaviors are compared with the surfaces of bulk materials (Al_2O_3, BaF_2, CaF_2, Ge, KBr, LiF, MgF_2, NaCl, Quartz, Si, ZnS, ZnSe, and different silica glasses). Tabulated values of results are presented and discussed. © 2013 Optical Society of America

OCIS codes: (310.0310) Thin films; (140.3330) Laser damage; (320.2250) Femtosecond phenomena.
http://dx.doi.org/10.1364/AO.53.00A186

1. Introduction

The laser damage resistance of optical components is a primary consideration in the development of high-power ultrashort pulse lasers. In these laser systems, there are technological challenges to produce specific multilayer optical coatings that can limit pulse lengthening and spectral distortion, and exhibit high laser-induced damage thresholds (LIDTs). Progress on this particular topic requires experimental data on the LIDTs of optical coating materials and a fundamental knowledge of laser damage mechanisms. Despite common characteristics with bulk materials, the laser damage of dielectric thin films has peculiarities that need to be taken into account: specific optical, mechanical, thermal, and electronic properties affecting the resistance of components under laser exposition, these properties being dependent on the deposition conditions. For practical applications, as for fundamental research in this field, experimental measurements of the LIDTs of optical materials are of key importance. These data can be used for the design of multilayer coatings or for comparison with theoretical models. However, in only a few studies dedicated to the sub-picosecond regime have different optical materials been investigated and compared: Stuart *et al.* [1] have reported LIDTs for high bandgap materials (SiO_2, CaF_2, MgF_2, BaF_2, and LiF) and Simanovskii *et al.* [2] have also studied high bandgap materials (CaF_2, MgF_2, BaF_2, and LiF) and ZnSe. In the study of Mero *et al.* [3] dielectric optical coatings were investigated (TiO_2, Ta_2O_5, HfO_2, Al_2O_3, and SiO_2), and in the study of Watanabe *et al.* [4] intermediate bandgap materials were studied ($SrTiO_3$, ZrO_2, $LaAl_2O_3$, MgO, and Al_2O_3). Nevertheless, the results are difficult to compare because laser damage measurements were made in different conditions, which can lead to discrepancies. Therefore, the objective of the present paper is to report on an extensive study of optical materials in bulk and thin film forms that have been characterized

1559-128X/14/04A186-11$15.00/0
© 2014 Optical Society of America

and damage-tested in similar conditions. A large part of the results in the case of coatings has been reported in different published works from our group [5–12]; however, the interest of the present paper is to compare and discuss all these experimental results on the same basis, using scaling laws that will be described. Additionally, these data have been completed with other coating and bulk materials (see Tables 1, 2, and 3). Particularly, the relationship between the damage resistance and the bandgap on the one hand and on the refractive index on the other, are investigated. The first dependency is, indeed, of main interest for the study of the physical processes involved [3] and the former is of interest for the design of laser damage-resistant multilayer coatings [14]. In this paper, however, we restrict our investigations to the case of single-shot irradiation. In the case of multiple pulses, the damage threshold is decreasing with the number of pulses, an effect called incubation, or fatigue. This decrease of the damage resistance is directly related to the number of incident pulses, but also on other irradiation parameters, such as pulse duration, as observed in IBS oxide coatings [15,16] and, possibly, repetition rate. As the process involved is dependent on native and laser-induced electronic defects, extensive systematic studies are also needed on this point to study these behaviors for different coating materials and deposition processes, but this is beyond the scope of this paper.

2. Materials and Methods

A. Samples

Dielectric films of different oxides and fluorides that are available for optical coatings - AlF_3, Al_2O_3, HfO_2, MgF_2, Nb_2O_5, Sc_2O_3, SiO_2, Ta_2O_5, TiO_2, Y_2O_3 and ZrO_2—were investigated. They were produced with various state-of-the-art deposition techniques: Electron Beam Deposition (with and without Ion Assistance), Ion Beam Sputtering or Magnetron Sputtering. These samples were produced at the Institut Fresnel, the CILAS company and the REOSC company. Mixtures of oxides and fluorides made by the codeposition of two source materials were also studied (deposited by the Laser Zentrum Hannover, Germany, and the Center for Physical Sciences and Technology, Lithuania): mixtures of AlF_3–Al_2O_3, Al_2O_3–SiO_2, HfO_2–SiO_2, Nb_2O_5–SiO_2, Sc_2O_3–SiO_2, Ta_2O_5–SiO_2, and ZrO_2–SiO_2. These materials are of particular interest for laser applications, their most important property being the ability to tailor the optical constants (refractive index and bandgap energy). The mixture coatings were fabricated in an ion beam sputtering process, applying a zone target assembly. A more detailed description of the coating plants and some aspects of the deposition process are published in [6,9,12,17]. Results obtained on metallic films (Ag, Pt) [10] are also reported.

All coatings were deposited on fused silica substrates, except AlF_3–Al_2O_3 samples that were deposited on MgF_2 substrates [12] and metallic films that were deposited on polymers. Some experiments were conducted on coatings deposited on substrates with different polishing grades and no distinguishable difference in the intrinsic LIDT between samples deposited on the substrates with the different polishing qualities were found (Ref. [9]).

The bulk materials come from different vendors, as windows for laser applications (CVI-Melles Griot, Edmund Optics, Eksma). Wide-gap, narrow-gap, and semiconductor materials were selected to compare optical coatings with their bulk counterparts and to extend the range of investigated materials: Al_2O_3, BaF_2, CaF_2, Ge, KBr, LiF, MgF_2, NaCl, Quartz, Si, ZnS, ZnSe, and different silica glasses.

All coating samples, and some bulk samples, have been characterized with spectrophotometry at close to normal incidence to determine their optical properties. In the case of thin films, the refractive indices, extinction coefficients, and physical thicknesses were determined from the fit of transmittance and reflectance measurements in the low-absorptance spectral region using numerical methods. The optical bandgap values were determined from the absorption coefficient by plotting $(\alpha E)^{1/2}$ as a function of the photon energy and extrapolating the linear curve progression. For bulk samples, the refractive indices were taken from tabulated data [18] and the optical bandgap values were either determined from measurements, extracted from tabulated data [18], or provided by the vendor. It was noticed that, depending on the quality of the samples, the bandgaps could be very different from the reported data and, although it was not possible to do it for all samples in this study, these measurements are useful for the interpretation of laser damage measurements (i.e., the nonlinear ionization processes are directly dependent on the optical bandgap value). The details of the measured properties of the samples (refractive indices, thicknesses, optical bandgaps) and other data can be found in Tables 1,2, and3. A summary of the samples' properties is given in Fig. 1, as a plot of refractive index versus optical bandgap.

In the case of bulk materials, the data can be fitted with the following expression (black line on Fig. 1):

$$n^2 = 1 + \frac{12.5}{E_g}, \tag{1}$$

with E_g the bandgap in electron volt. The expression that is obtained for a large range of bandgap values can be compared with other gap-refractive index relations and based on simple physical models [19]. For instance, the relationship proposed by Moss for the case of semiconductor materials [20] is $n^4 E_g = 95$ eV. When applied to our measurements, the evolution of refractive index versus bandgap, predicted by the Moss rule (gray dotted line on Fig. 1), compares well to our experiments up to 5 eV and then overestimates the data for higher bandgaps. At the opposite end, the model of Herve

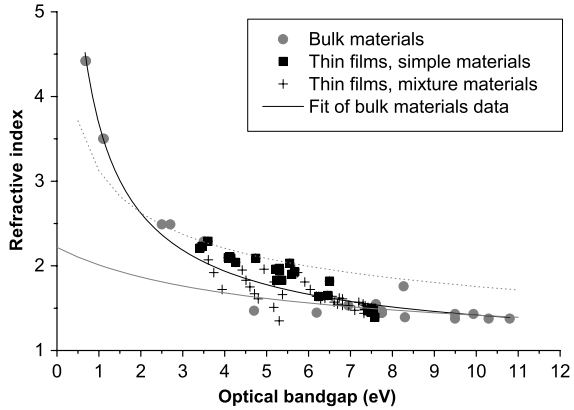

Fig. 1. Refractive indices at 1030 nm plotted as a function of optical bandgap values for the different dielectric and semiconductor samples under study. Data have been obtained from spectrophotometric measurements. The black line is a fit of bulk data. The dotted gray line is a plot of the Moss relation [20] and the solid gray line is a plot of the Herve and Vandamme relation [21].

and Vandamme [21] ($n^2 = 1 + 13.6/(E_g + 3.47)$) is accurate for high bandgap materials and shows strong deviations with experiments for semiconductors. In the intermediate range between semiconductors and high-bandgap materials (fluorides), there is some dispersion of refractive index values, particularly for mixture materials, and the two previously cited relations can be considered as the low and high boundary limits.

B. Measurements of Single-Shot Laser Damage Resistance

The single-shot laser damage resistance of the samples has been measured at 1030 nm with a commercial diode-pumped ytterbium-amplified laser operating in the sub-picosecond regime (500 fs), with the experiment and procedures described in detail in Ref. [7]. All the samples have been tested at normal incidence, with the surface to be tested facing the incoming beam (front face testing), in linear polarization with a beam diameter in the range of 50–60 μm at $1/e$, depending on the test campaign. The oscillator, amplifier, and compressor of the laser source have been realigned and optimized several times during the acquisition of the data reported in this paper. This implies that the measurements were not done under exactly the same conditions. In particular, the pulse duration and spot size were not the same for all the tested samples. The effective spot size, as defined in the ISO standard [22], is used for fluence determination; therefore, the consequences of spot size variations on the fluence are implicitly taken into account. The pulse duration, however, varied between 375 fs and 600 fs and a correction of the results is necessary to analyze the results. Therefore, to compare the results on the same basis (arbitrarily set to 500 fs), we applied the scaling law determined by Mero *et al.* in Ref. [3]: the dependence of the breakdown threshold fluence F_{th} on pulse duration t_p was found to be $F_{\mathrm{th}} \propto t_p^k$, with $k \approx 0.3$. This result was independent of the material in the mentioned work and, interestingly, this scaling law is in agreement with several works in which the pulse duration dependence of F_{th} was studied. By analyzing different published data we determined $k \approx 0.25$ for fused silica and $k \approx 0.35$ for borosilicate in the work of Lenzner *et al.* [23], $k \approx 0.26$ for borosilicate in the work of Kautek *et al.* [24], $k \approx 0.2$ for FS in the work of Tien *et al.* [25], and $k \approx 0.3$ in the work of Sanner *et al.* [26]. In the work of Stuart *et al.* [1], however, we found $k \approx 0.1$ for FS and CaF_2; however, in this case, multiple pulses by site were involved, as opposed to single shots in the other mentioned works. All the results given in this paper are scaled to 500 fs, but have been measured between 375 and 600 fs. Other sources of error can contribute to deviation in the determination of fluence: damage detection that is linked to the setting of the observation system, the operator, slow evolution of the calorimeter and pyrometer used in the experiment. The error budget of the absolute fluence determination is estimated to be less than ±10%, even if the relative fluence can be measured with an accuracy of ±1% [7]. In Fig. 2, we present an example of repetitive measurements made on a time scale of several years on 2 samples (single layer coatings).

To compare the LIDT values reported in this paper with other published data, we have investigated the results of several LIDT measurements that were made on the surface of fused silica, the most widely studied dielectric material in the literature. Only experiments involving single shots were selected since incubation effects occur for multiple pulses, which can make the results noncomparable. Also, only results between 100 fs and 1 ps were selected for our experimental conditions because they are in the range where physical mechanisms should be similar. The results found by different groups at 800 nm and 1030/1053 nm are plotted in Fig. 3, along with the same results rescaled at 500 fs with the scaling law described before for comparison. No wavelength scaling law was applied to compare the results at 800 and 1030/1053 nm since the photon

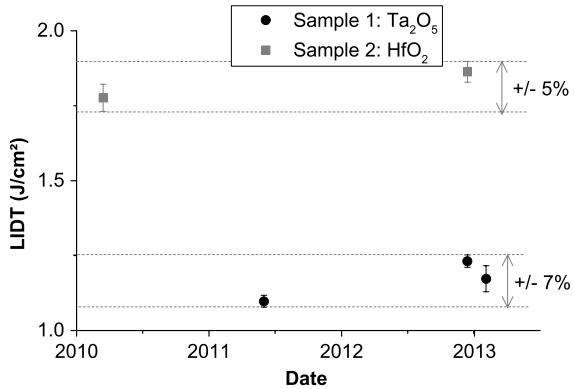

Fig. 2. Comparison of the LIDT measurements made on 2 samples (Ta_2O_5 and HfO_2 single layer coatings) through the years. The 2 samples have been stocked in ambient conditions, enclosed in unsealed individual polypropylene boxes between the tests.

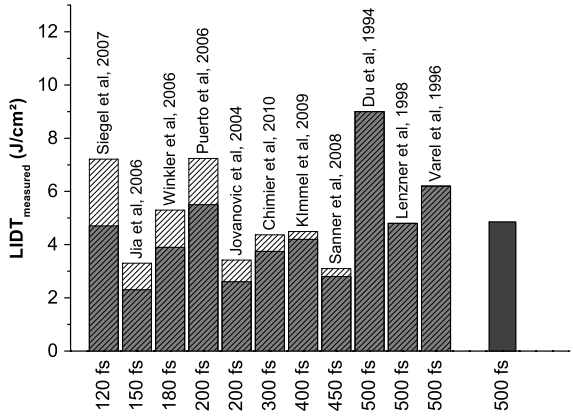

Fig. 3. Comparison of the LIDT measured by different groups on the surface of fused silica samples at 800 or 1053 nm. Measurements at the pulse duration of the experiments are given (dashed bars) and also rescaled values, with the scaling law given in the text for comparing the results at 500 fs (gray bars). Data are extracted from references [23,36–35]. The present measurement is given on the right (dark gray bar).

energies are very close (1.5 and 1.2 eV) and no noticeable difference was found between the two wavelengths in studies where the wavelength dependency was investigated [36].

The different values are found to be in the range of 2–9 J/cm^2, with a mean value around 5.4 J/cm^2. The discrepancy in the results of the groups may be due to a number of reasons. The LIDT can indeed be the subject of large differences, depending on the damage test procedure, damage criterion, damage detection, and laser stability. Another possible explanation may be that, since the tested fused silica samples were not the same, depending on the fabrication and polishing processes used, the samples may have different properties. In our case, the damage threshold of the fused silica sample is 4.85 J/cm^2.

3. Results and Discussion

To present the results, we will make the distinction between the "internal" LIDT and "measured" LIDT of the samples. The internal, or intrinsic LIDT of the material corresponds to the measured data that are rescaled to take into account the electric field distribution in the sample, using the following definition:

$$\mathrm{LIDT}_{\mathrm{internal}} = |E_{\max}/E_{\mathrm{inc}}|^2 \mathrm{LIDT}_{\mathrm{measured}}, \qquad (2)$$

with $E_{\max}/E_{\mathrm{inc}}$ the ratio of the maximum of the electric field distribution in the samples to the incident field. This correction factor is applied to the coating samples, since there are interference effects in the film, and also to the bulk samples to compare all samples on the same basis (in this case, $E_{\max}$ is the value on the surface). Note that, in the case of a half-wave layer, bulk and coating data could be compared directly, since the ratio is the same.

A. Films of Simple Oxides and Fluorides

The LIDTs measured on the different dielectric thin film samples are reported in Figs. 4 and 5. The LIDTs are plotted on Fig. 4 as a function of the measured gap, since the main property that drives laser damage resistance is the optical bandgap. For applications, a crucial material parameter for the design of multilayer optical components is the refractive index. Figure 5 describes the LIDTs and their relation to the refractive index.

A linear dependency of the LIDT with respect to the bandgap value has been observed on IBS oxide films (Al_2O_3, HfO_2, SiO_2, Ta_2O_5, TiO_2) and described using a phenomenological model by Mero *et al.* [3]. This linear dependency is also observed in our experiments on an extended range of materials and manufacturing techniques and our results are in good agreement with the previously cited phenomenological law. For the cases of HfO_2, Nb_2O_5, Sc_2O_3, SiO_2, and Ta_2O_5, the dispersion of results is within the error margin given in the previous

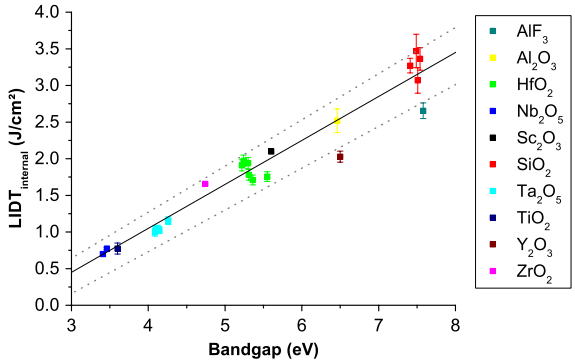

Fig. 4. LIDTs of optical thin film materials tested in single-shot at 500 fs and 1030 nm as a function of the measured optical bandgaps. The values are given as the internal LIDT, i.e., by taking into account the electric field distribution in the film. Each point corresponds to a different sample. The plain and dotted lines correspond to the plot of Eq. (3) with its error margin. See Table 2 for data and references.

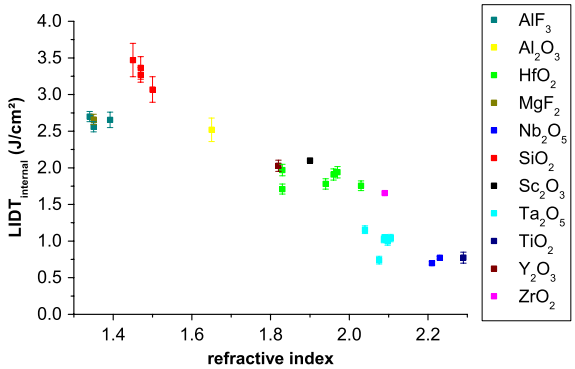

Fig. 5. Internal LIDTs of thin film materials tested in single-shot at 500 fs and 1030 nm, as a function of their refractive index at 1030 nm. This figure includes more samples than Fig. 4; i.e., samples for which the optical bandgap was not determined. See Table 2 for data and references.

Table 1. Summary of Results for the Surfaces of Bulk Materials[a]

Bulk Materials					
Material	Refractive Index (at 1030 nm)	Bandgap (eV)	Measured LIDT (J/cm^2)	Internal LIDT (J/cm^2)	Remarks and References
Al_2O_3	1.76	8.3	5.36 ± 0.2	2.79 ± 0.11	
BaF_2	1.47	4.7*	2.91 ± 0.09	1.91 ± 0.06	*Bandgap value given by the vendor
CaF_2 a	1.43	9.5*	5.17 ± 0.14	3.50 ± 0.09	*Bandgap value given by the vendor
CaF_2 b	1.43	9.93	6.38 ± 0.23	4.32 ± 0.16	
Ge a	$4.42 + i0.15$	0.7*	0.24 ± 0.04	0.031 ± 0.005	*From Ref. [18]
Ge b	$4.42 + i0.15$	0.7*	0.33 ± 0.02	0.043 ± 0.003	*From Ref. [18]
Infrasil	1.45	6.2	4.16 ± 0.12	2.75 ± 0.08	
KBr	1.55	7.6	3.31 ± 0.1	2.02 ± 0.06	
LiF	1.39	8.3*	4.43 ± 0.11	3.11 ± 0.08	*Bandgap value given by the vendor
MgF_2 a	1.38	10.8	6 ± 0.11	4.24 ± 0.08	
MgF_2 b	1.38	10.3*	5.99 ± 0.09	4.23 ± 0.08	*Bandgap value given by the vendor
MgF_2 c	1.38	9.5*	4.8 ± 0.12	3.38 ± 0.09	*Bandgap value given by the vendor
NaCl	1.53	6.95	2 ± 0.22	1.24 ± 0.14	
Si a	3.5	1.1*	0.91 ± 0.05	0.18 ± 0.01	
Si b	3.5	1.1*	0.55 ± 0.04	0.11 ± 0.008	*From Ref. [18]
SiO_2 a (Suprasil)	1.45	7.75	4.6 ± 0.12	3.04 ± 0.08	
SiO_2 b (UVFS)	1.45	7.2*	4.85 ± 0.17	3.21 ± 0.11	*Bandgap value given by the vendor
SiO_2 c (Quartz)	1.45	7.75*	5.36 ± 0.08	3.54 ± 0.05	*Estimated
SiO_2 d (C7980)	1.45	7.75*	4.42 ± 0.22	2.92 ± 0.15	*Estimated
ZnS a	2.29	3.5*	1.08 ± 0.02	0.40 ± 0.008	*From Ref. [18]
ZnS b	2.29	3.5*	1.10 ± 0.02	0.41 ± 0.008	*From Ref. [18]
ZnSe a	2.49	2.7*	0.53 ± 0.08	0.17 ± 0.03	*From Ref. [18]
ZnSe b	2.49	2.5*	0.53 ± 0.06	0.18 ± 0.02	*Bandgap value given by the vendor

[a]LIDT values are given at 500 fs, 1030 nm, single-pulse irradiation (see text for details). The optical bandgap values indicated with "*" have been extracted from references. Other bandgap values have been measured.

section. For Y_2O_3 and AlF_3, the damage threshold is lower than the value that can be expected from the linear tendency. The relatively low dispersion of results is remarkable because the samples have very different intrinsic properties that can drive the damage process: electronic properties, such as the band structure and the density of defect states), or other physical properties, such as the adherence of the film, the thermal properties, or the density.

At 500 fs, 1030 nm, the following empirical description was found [8,37]:

$$\mathrm{LIDT} = 0.6(\pm 0.03\ \mathrm{Jcm^{-2}\ eV})E_g - 1.35(\pm 0.2\ \mathrm{Jcm^{-2}}). \quad (3)$$

This linear behavior can be explained by taking into account the physical processes involved in the initial ionization damage event (photo and impact ionization) and their dependency on the bandgap. Comparison with simple physical-based models were done in Ref. [8] and a good description of the experimental results was obtained.

The optical bandgap and refractive index values are related, as described in the first section. For the case of dielectric thin films of simple materials, the relationship between bandgap and refractive index has a linear behavior, as observed in Fig. 1. As a consequence, there is a linear tendency between LIDT and refractive index, as observed in Fig. 5. For oxide materials, a dispersion of results is observed that is related to the dependency of the refractive index on both the density and the optical bandgap; these two properties being dependent on the manufacturing process. In the case of fluoride materials, which have a lower refractive index than silica, the measured LIDTs are quite low compared with the values that could be expected from the tendency of oxide materials. Their LIDTs are significantly lower that the silica samples.

The properties of films are closely related to their deposition parameters. To illustrate the influence of deposition technique and parameters on laser damage resistance in the sub-picosecond regime, we have plotted in Fig. 6 the comparative results of 11 different HfO_2 samples, each one made with a different deposition technique and/or deposition parameter. These samples are produced by 5 different manufacturers. One of the samples has a very low damage threshold compared with the other ones

Table 2. Summary of Results for Films of Simple Oxides and Fluorides[a]

Simple Films				
Material	Refractive Index (at 1030 nm)	Bandgap (eV)	Internal LIDT (J/cm^2)	Deposition Technique and References
Ag	0.28 + i7.5 [18]		0.094 ± 0.011	RF sputtering [10]
Al_2O_3	1.65	6.46	2.52 ± 0.16	EBD [11]
AlF_3 b	1.34	n.m.	2.7 ± 0.07	
AlF_3 c	1.35	n.m.	2.56 ± 0.07	
HfO_2 a	1.83	5.24	1.97 ± 0.08	EBD [11]
HfO_2 b	1.83	5.36	1.71 ± 0.07	EBD [11]
HfO_2 c	1.96	5.22	1.91 ± 0.08	EBD [11]
HfO_2 d	1.94	5.31	1.78 ± 0.07	EBD [11]
HfO_2 e	1.97	5.3	1.94 ± 0.08	EBD-IAD [11]
HfO_2 f	2.06	n.m.	1.31 ± 0.05	DIBS [5]
HfO_2 g	2.13	n.m.	1.74 ± 0.07	RLVIP [5]
HfO_2 h	1.87	n.m.	1.89 ± 0.08	EBD [5]
HfO_2 i	1.86	n.m.	2.02 ± 0.08	EBD [5]
HfO_2 j	n.m.	n.m.	1.80 ± 0.05	EBD-IAD
MgF_2	1.35	n.m.	2.66 ± 0.07	
Nb_2O_5 a	2.23	3.46	0.77 ± 0.02	IBS [6]
Nb_2O_5 b	2.21	3.41	0.7 ± 0.03	EBD-IAD [6]
Pt	3.55 + i5.92		0.015 ± 0.001	RF sputtering [10]
Sc_2O_3 b	1.9	5.6	2.1 ± 0.02	[11]
SiO_2 a	1.48	n.m.	4.28 ± 0.07	IBS [6]
SiO_2 b	1.46	7.49	3.15 ± 0.35	[11]
Ta_2O_5 a	2.09	4.10	1.05 ± 0.04	DIBS
Ta_2O_5 b	2.11	4.13	1.04 ± 0.05	DIBS
Ta_2O_5 c	2.09	4.15	1.02 ± 0.05	DIBS
Ta_2O_5 d	2.10	4.09	1.00 ± 0.05	DIBS
Ta_2O_5 e	2.08	n.m.	0.74 ± 0.05	Magnetron sputtering
TiO_2	2.29	3.6	0.77 ± 0.08	EBD [11]
Y_2O_3	1.82	6.5	2.03 ± 0.08	EBD [11]
ZrO_2	2.09	4.74	1.66 ± 0.02	EBD [11]

[a]LIDT values are given at 500 fs, 1030 nm, single-pulse irradiation (see text for details). For previously published results, the details of the fabrication, laser damage testing conditions, and results, as with the refractive indices and optical bandgap determinations, can be found in the cited references ("n.m.": not measured).

and this was correlated to an increase of absorption that can be linked to oxygen deficiency and a nonstoichiometric film. Another sample has a relatively low LIDT (DIBS sample) and was also correlated to a higher absorption than other samples (see Ref. [38] where the sample characterization is detailed). For all other samples, which were produced with the best parameters determined by the manufacturers, it can be seen that the measured LIDTs are within the margin of error of the experiment. On this material, which is one of the most important high-index materials used in the production of optical multilayer coatings for laser applications, the highest LIDT can be achieved after optimization of the deposition parameters and the intrinsic limits of the material are reached.

B. Surfaces of Bulk Materials

Thin films and the surfaces of bulk sample LIDTs are compared to determine if, for any material, the resistance of the film reaches the resistance of the bulk. The LIDTs measured for the different bulk samples are reported in Fig. 7, with the results plotted as a function of optical bandgap. The previous results obtained on the thin film samples are also reported on this figure, for comparison. To be more exhaustive, the thresholds of two metals (platinum and silver thin films, for which details can be found in Ref. [10]), are also given on this figure, indicated with a bandgap of 0 eV. We recall the differences in the reported data, where the thresholds are given as "internal" threshold, i.e., taking into account the electric field value at the surface of the materials, to make thin film and bulk material results comparable.

The LIDTs for the case of thin films and the surfaces of bulk materials follow the same evolution as a function of bandgap and are comparable, with the exception of NaCl and KBr samples that have a low LIDT compared with the mean tendency. These two materials were tested in the air, whereas, they are known to be hygroscopic and the low LIDT could be due to modifications of the surface quality due to water absorption. For all other tested materials, the results have the same linear trend of LIDT versus bandgap. The dispersion of the results around this tendency can be due to the very different physical properties of the tested materials that can influence the damage process (electronic, thermal, mechanical,

Table 3. Summary of Results for Films of Mixture Materials (IBS)[a]

Mixture Films				
Material	Refractive Index (at 1030 nm)	Bandgap (eV)	Internal LIDT (J/cm^2)	References
Al_2O_3–AlF_3	1.64	6.24	1.97 ± 0.03	[12]
Al_2O_3–AlF_3	1.61	6.39	3.06 ± 0.12	[12]
Al_2O_3–AlF_3	1.57	6.61	3.31 ± 0.12	[12]
Al_2O_3–AlF_3	1.55	6.69	3.45 ± 0.12	[12]
Al_2O_3–AlF_3	1.53	6.81	3.22 ± 0.12	[12]
Al_2O_3–AlF_3	1.48	7.1	3.82 ± 0.15	[12]
Al_2O_3–AlF_3	1.44	7.32	3.88 ± 0.18	[12]
Al_2O_3–AlF_3	1.41	7.5	4.68 ± 0.17	[12]
Al_2O_3–AlF_3	1.39	7.58	2.78 ± 0.12	[12]
Al_2O_3–SiO_2	1.65	6.46	2.52 ± 0.16	[17]
Al_2O_3–SiO_2	1.64	6.56	2.63 ± 0.17	[17]
Al_2O_3–SiO_2	1.62	6.73	2.75 ± 0.15	[17]
Al_2O_3–SiO_2	1.61	6.81	2.73 ± 0.16	[17]
Al_2O_3–SiO_2	1.57	7.20	2.73 ± 0.14	[17]
Al_2O_3–SiO_2	1.55	7.30	2.60 ± 0.18	[17]
Al_2O_3–SiO_2	1.53	7.35	2.81 ± 0.17	[17]
Al_2O_3–SiO_2	1.51	7.42	2.82 ± 0.17	[17]
Al_2O_3–SiO_2	1.50	7.49	2.57 ± 0.15	[17]
Al_2O_3–SiO_2	1.50	7.51	3.07 ± 0.17	[17]
HfO_2–SiO_2	2.03	5.55	1.76 ± 0.06	[13]
HfO_2–SiO_2	1.96	5.67	1.75 ± 0.07	[13]
HfO_2–SiO_2	1.92	5.74	1.85 ± 0.07	[13]
HfO_2–SiO_2	1.81	5.91	2.07 ± 0.08	[13]
HfO_2–SiO_2	1.72	6.04	2.24 ± 0.07	[13]
HfO_2–SiO_2	1.64	6.19	2.53 ± 0.07	[13]
HfO_2–SiO_2	1.60	6.29	2.62 ± 0.09	[13]
HfO_2–SiO_2	1.53	6.96	2.88 ± 0.07	[13]
HfO_2–SiO_2	1.49	7.33	3.10 ± 0.07	[13]
HfO_2–SiO_2	1.47	7.54	3.36 ± 0.15	[13]
Nb_2O_5–SiO_2	2.23	3.46	0.77 ± 0.02	[6]
Nb_2O_5–SiO_2	2.07	3.61	1.03 ± 0.02	[6]
Nb_2O_5–SiO_2	1.92	3.74	1.38 ± 0.04	[6]
Nb_2O_5–SiO_2	1.72	3.94	2.10 ± 0.03	[6]
Nb_2O_5–SiO_2	1.48	7.5*	4.27 ± 0.07	[6]
Sc_2O_3–SiO_2	1.93	5.67	3.11 ± 0.07	[9]
Sc_2O_3–SiO_2	1.87	5.78	3.35 ± 0.07	[9]
Sc_2O_3–SiO_2	1.84	5.82	3.53 ± 0.07	[9]
Sc_2O_3–SiO_2	1.77	6.02	3.60 ± 0.07	[9]
Sc_2O_3–SiO_2	1.71	6.18	3.40 ± 0.07	[9]
Sc_2O_3–SiO_2	1.61	6.44	3.26 ± 0.07	[9]
Sc_2O_3–SiO_2	1.54	6.69	2.95 ± 0.07	[9]
Sc_2O_3–SiO_2	1.50	6.92	3.17 ± 0.07	[9]
Sc_2O_3–SiO_2	1.49	7.09	2.95 ± 0.07	[9]
Sc_2O_3–SiO_2	1.47	7.41	3.19 ± 0.05	[9]
Ta_2O_5–SiO_2	2.04	4.26	1.15 ± 0.05	[17]
Ta_2O_5–SiO_2	1.95	4.42	1.34 ± 0.07	[17]
Ta_2O_5–SiO_2	1.83	4.51	1.74 ± 0.07	[17]
Ta_2O_5–SiO_2	1.75	4.60	1.96 ± 0.15	[17]
Ta_2O_5–SiO_2	1.67	4.71	2.36 ± 0.11	[17]
Ta_2O_5–SiO_2	1.61	4.80	2.78 ± 0.13	[17]
Ta_2O_5–SiO_2	1.51	5.17	3.61 ± 0.23	[17]
Ta_2O_5–SiO_2	1.48	7.34	3.70 ± 0.24	[17]
Ta_2O_5–SiO_2	1.46	7.49	3.72 ± 0.24	[17]
Ta_2O_5–SiO_2	1.45	7.49	3.47 ± 0.23	[17]
ZrO_2–SiO_2	2.09	4.74	1.66 ± 0.015	[6]
ZrO_2–SiO_2	1.96	4.94	1.96 ± 0.03	[6]
ZrO_2–SiO_2	1.81	5.18	2.46 ± 0.02	[6]
ZrO_2–SiO_2	1.66	5.38	3.11 ± 0.06	[6]
ZrO_2–SiO_2	1.48	7.5*	4.27 ± 0.07	[6]

[a]LIDT values are given at 500 fs, 1030 nm, single-pulse irradiation (see text for details). For previously published results, the details of the fabrication, laser damage testing conditions, and results, as with the refractive indices and optical bandgap determinations, can be found in the cited references ("*": estimated).

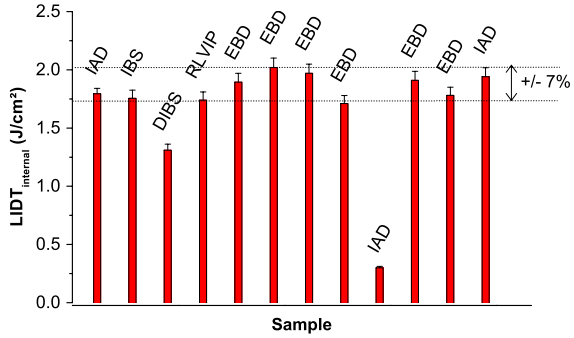

Fig. 6. Laser-induced damage threshold for 11 different HfO_2 samples. The deposition technique is indicated for each sample. See Table 2 for data and references.

and surface properties). In the case of oxide coatings, the LIDT of films and the surface of bulk materials are comparable, which means that the intrinsic limits of the materials are reached and it seems difficult to improve their LIDT with the optimization of the deposition parameters (as opposed to the case of the nanosecond regime). The highest damage resistance for oxides is obtained for silica, and the value is the same for materials in thin film or bulk form. In the case of Al_2O_3, we also observe the same value for thin film and bulk form. For fluoride materials with high optical bandgaps (CaF_2, MgF_2), a threshold 20% higher than silica is observed for bulk materials (for the best samples). Such high values are not observed on the tested samples for fluoride thin film and more progress is required to obtain film materials with higher damage thresholds.

C. Binary Mixtures

Composite or mixture films can be produced by the simultaneous deposition of several materials with the main deposition technologies used in optical coating production [39]. These films are of interest for their intrinsic properties and for the design of multilayer stacks. Indeed, by incorporating a small amount of one material in another one, it is possible to change the microstructural properties of the film and reduce the residual stress or the roughness (e.g., SiO_2 in ZrO_2 [6,40], SiO_2 in TiO_2 [41], SiO_2 in Gd_2O_3 [42], and Ta_2O_5 in SiO_2 [43]), or to improve the optical homogeneity [39]. For high-power femtosecond applications, these materials may make it possible to tune the optical constants and produce continuous spatial variations of the refractive index. With an adapted design, based on an optimization of the electric field distribution, the use of mixture materials can lead to subsequent enhancement of the LIDT of multilayer systems compared with the use of pure material systems [14]. Such approaches are based on the precise knowledge of the damage behavior of the films as a function of their composition and the ability to predict this behavior. The LIDT of mixture coatings in the femtosecond regime has, however, not been the object of extensive studies and we report in Figs. 8–10 the results of different experimental studies on laser damage resistance in binary mixtures. Results are expressed as laser damage resistance evolution as a function of the bandgap (Fig. 8), the material content, i.e., percentage of low index material in the mixture (Fig. 9), and the refractive index (Fig. 10).

By comparing the evolution of LIDT versus optical bandgap for the case of mixture coatings with the case of simple materials (Fig. 8) we can observe a very different behavior. The linear evolution is not followed by the mixture coatings and a more complex behavior is evidenced in this figure. Starting from the high-index materials (Nb_2O_5, ZrO_2, HfO_2, Al_2O_3, Ta_2O_5, Sc_2O_3), with the lowest bandgap value, we observed, with a more or less pronounced effect, a linear increase of the LIDT versus bandgap, but with a higher slope than for the case of simple materials. This linear evolution is, however, restricted to a range of bandgap values and above that range we

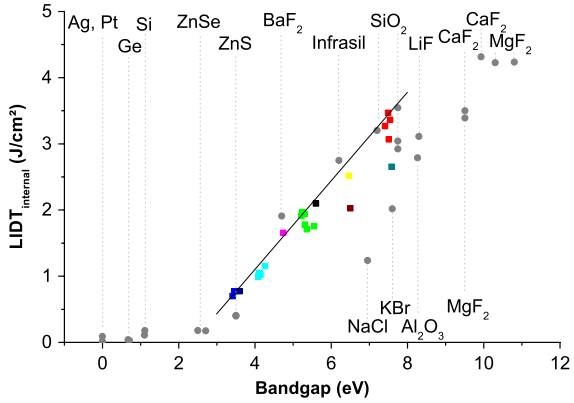

Fig. 7. LIDTs of optical thin film materials (color filled squares, with color code similar to previous figures) and bulk materials (gray filled circles) tested in single-shot at 500 fs and 1030 nm, as a function of the optical bandgaps (measured or estimated). The values are expressed as the internal LIDT. The black line is reported from Fig. 4. See Table 1 for data and references.

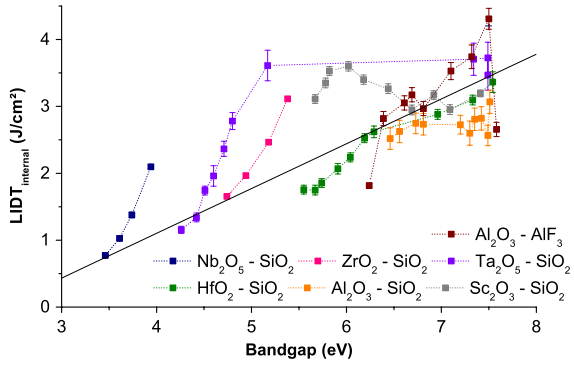

Fig. 8. Internal LIDTs of single layers of mixture materials tested under single-shot irradiation at 500 fs and 1030 nm, as a function of the measured absorption gaps. The labels (e.g., Nb_2O_5–SiO_2) are an indication of the composition of the film (co-deposition of silica and niobia); however, the films could be off-stoichiometric. The dotted lines are guides for the eyes and they link the samples of the same set of deposition. The black line corresponds to the tendency observed for simple materials [Eq. (3)]. See Table 3 for data and references.

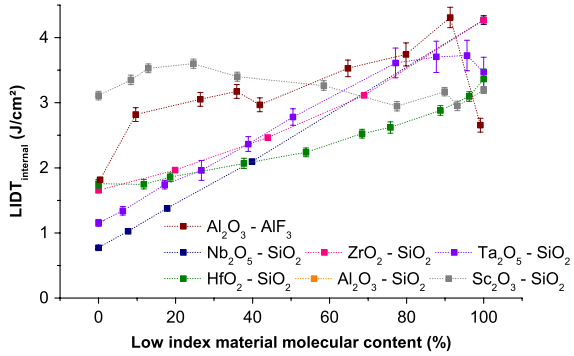

Fig. 9. Internal LIDTs of single layers of mixture materials tested under single-shot irradiation at 500 fs and 1030 nm, as a function of the low-index material molecular content. For instance, the sample 55% HfO_2–SiO_2 should be composed of 55% of SiO_2 and 45% of HfO_2 if the film is perfectly stoichiometric. In the case of the Al_2O_3–AlF_3 samples, the low-index material is AlF_3.

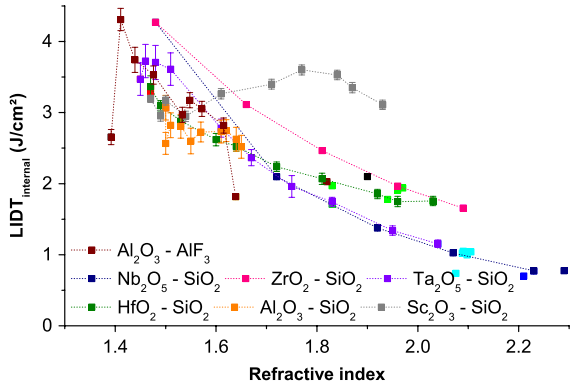

Fig. 10. Internal LIDTs of single layers of mixture materials tested under single-shot irradiation at 500 fs and 1030 nm, as a function of the refractive index at 1030 nm.

observe a saturation, or a decrease of the LIDT, with the limited number of samples that were tested. This linear evolution on a restricted range was also observed in the work of Nguyen *et al.* [44] on TiO_2–SiO_2 mixture coatings. The bandgap, with the evaluation method described in Section 2, is certainly not the adapted parameter in the case of mixture coatings to quantify the damage resistance of the films. On the basis of simple models, based on the rate equation [1,45] to describe the damage initiation process, possible explanations of the higher LIDTs for a given bandgap value could be:

- a higher relaxation rate of electrons from the conduction band to lower electronic states due to a high density of trapping defects in these films
- a higher effective electron mass related to an evolution of the band structure.

An in-depth understanding of such behaviors would require some characterization about their electronic structure with, for instance, tools used in the field of high-k dielectrics for microelectronics (e.g., electron energy spectroscopies).

We have also plotted the results as a function of the molecular fraction of the low-index material that comprises the mixture film (Fig. 9). This molecular fraction was obtained by using a Lorentz–Lorentz effective medium theory model to obtain the volumetric fraction of each material (e.g., see Ref. [6]) and then the molecular fraction was obtained based on the density and molar weight of each of the contents. Using this parameter, we can obtain a more consistent description of the LIDT with the physical parameter of the film. Indeed, in the cases of HfO_2–SiO_2, Nb_2O_5–SiO_2, Ta_2O_5–SiO_2, and ZrO_2–SiO_2, there is a direct proportionality of the LIDT with the molecular content, which was not the case for its dependence on the bandgap. In the cases of Al_2O_3–SiO_2 and Sc_2O_3–SiO_2, the difference of LIDT values between the low- and high-index material is too low to observe a consistent evolution. The material composition calculated with this approach is, therefore, a good parameter to estimate the damage resistance of a mixture material, based on the knowledge of the LIDT of each of the primitive materials.

If we analyze now the LIDT as a function of the refractive index of the mixture film (Fig. 10), we can observe that, with the exception of the Sc_2O_3–SiO_2 mixture, the behavior of the mixture films is the same as that of the simple films. The mixture materials fill the gaps between the simple thin film materials. In the case of the Sc_2O_3–SiO_2 mixture samples, a clear deviation from the general tendency is observed. This is associated with a change in the damage morphology, with the occurrence of more pronounced thermal effects when the Sc_2O_3 content is increased. The relatively high damage threshold compared with other materials makes Sc_2O_3–SiO_2 mixtures an interesting choice for producing high-index optical interference coatings for use in high-power applications in the femtosecond-pulse duration range. However, we must keep in mind that these results are obtained for single-pulse irradiation. For low refractive index materials, fluoride films exhibit quite a low damage threshold when compared with their bulk counterparts; however, by introducing a small amount of an oxide (Al_2O_3 in AlF_3 in the case shown in Fig. 8) notably improves the properties of the film and a high LIDT compared with silica can be obtained.

4. Conclusion

We have reported on an extensive experimental study on the laser damage resistance of thin films and bulk optical materials at 1030 nm, 500 fs. In the case of simple materials, a clear ranking can be established, based on their bandgap values and linear evolution of the LIDT, as observed in previous studies. The surfaces of bulk material and thin film materials were both found to have the same evolution and comparable laser damage resistance. Accordingly, the deposition parameters were found to be not very critical, at least for the single-shot irradiation conditions of these tests. In the case of mixture films, however, a more complex behavior

is observed that cannot be described by simple models (rate equation) or simple phenomenological laws based on the first-order dependency on the bandgap of the materials. In some cases (i.e., Sc_2O_3–SiO_2), the combination of the materials gives specific properties to the film and a very high damage threshold can be achieved. The results reported in this paper were, however, restricted to one particular condition (1030 nm, 500 fs, single-shot irradiation). Further studies using different irradiation parameters (wavelength, multishot irradiation) and using the same methodology will extend these threshold measurements for use in applications.

The results presented in this paper have been obtained thanks to the contributions of people involved in the preparation and characterization of the samples. The authors would like to acknowledge their support:

- D. B. Douti, B. Mangote, F. Lemarchand, C. Hecquet, and M. Lequime from Institut Fresnel, France
- M. Mende, H. Ehlers, L. Jensen, and M. Jupé, D. Ristau from Laser Zentrum Hannover, Germany
- A. Melninkaitis and V. Sirutkaitis from Laser Research Center, Lithuania
- A. Hervy and D. Mouricaud from REOSC company.

References and Notes

1. B. C. Stuart, M. D. Feit, S. Herman, A. M. Rubenchik, B. W. Shore, and M. D. Perry, "Nanosecond-to-femtosecond laser-induced breakdown in dielectrics," Phys. Rev. B **53**, 1749–1761 (1996).
2. D. M. Simanovskii, H. A. Schwettman, H. Lee, and A. J. Welch, "Midinfrared optical breakdown in transparent dielectrics," Phys. Rev. Lett. **91**, 107601 (2003).
3. M. Mero, J. Liu, W. Rudolph, D. Ristau, and K. Starke, "Scaling laws of femtosecond laser pulse induced breakdown in oxide films," Phys. Rev. B **71**, 115109 (2005).
4. F. Watanabe, D. G. Cahill, B. Gundrum, and R. S. Averback, "Ablation of crystalline oxides by infrared femtosecond laser pulses," J. Appl. Phys. **100**, 083519 (2006).
5. L. Gallais, B. Mangote, M. Zerrad, M. Commandré, A. Melninkaitis, J. Mirauskas, M. Jeskevic, and V. Sirutkaitis, "Laser-induced damage of hafnia coatings as a function of pulse duration in the femtosecond to nanosecond range," Appl. Opt. **50**, C178–C187 (2011).
6. A. Melninkaitis, T. Tolenis, L. Mazule, J. Mirauskas, V. Sirutkaitis, B. Mangote, X. Fu, M. Zerrad, L. Gallais, M. Commandré, S. Kicas, and R. Drazdys, "Characterization of zirconia and niobiasilica mixture coatings produced by ion-beam sputtering," Appl. Opt. **50**, C188–C196 (2011).
7. B. Mangote, L. Gallais, M. Zerrad, F. Lemarchand, L. H. Gao, M. Commandré, and M. Lequime, "A high accuracy femto-/picosecond laser damage test facility dedicated to the study of optical thin films," Rev. Sci. Instrum. **83**, 013109 (2012).
8. B. Mangote, L. Gallais, M. Commandré, M. Mende, L. Jensen, H. Ehlers, M. Jupé, D. Ristau, A. Melninkaitis, J. Mirauskas, V. Sirutkaitis, S. Kicas, T. Tolenis, and R. Drazdys, "Femtosecond laser damage resistance of oxide and mixture oxide optical coatings," Opt. Lett. **37**, 1478–1480 (2012).
9. M. Mende, S. Schrameyer, H. Ehlers, D. Ristau, and L. Gallais, "Laser damage resistance of ion-beam sputtered Sc_2O_3/SiO_2 mixture optical coatings," Appl. Opt. **52**, 1368–1376 (2013).
10. L. Gallais, E. Bergeret, B. Wang, M. Guerin, and E. Benevent, "Ultrafast laser ablation of metal films on flexible substrates," Appl. Phys. A, doi:10.1007/s00339-013-7901-2 (to be published).
11. A. Hervy, L. Gallais, D. Mouricaud, and G. Chériaux, "Electron-beam deposited materials for high-reflective coatings: Femtosecond LIDT," *Optical Interference Coatings*, OSA Technical Digest (Optical Society of America, 2013), paper FA.4.
12. M. Mende, I. Balasa, H. Ehlers, D. Ristau, D.-B. Douti, L. Gallais, and M. Commandré, "Correlation of optical properties and laser damage resistance for ion beam sputtered Al_2O_3/AlF_3 and Al_2O_3/SiO_2 mixture coatings," Appl. Opt., (submitted).
13. M. Jupé, M. Mende, C. Kolleck, D. Ristau, L. Gallais, and B. Mangote, "Measurement and calculation of ternary oxide mixtures for thin films for ultra short pulse laser optics," Proc. SPIE **8190**, 819004 (2011).
14. M. Jupé, M. Lappschies, L. Jensen, K. Starke, and D. Ristau, "Improvement in laser irradiation resistance of fs-dielectric optics using silica mixtures," Proc. SPIE **6403**, 64031A (2007).
15. M. Mero, B. Clapp, J. C. Jasapara, W. Rudolph, D. Ristau, K. Starke, J. Kruger, S. Martin, and W. Kautek, "On the damage behavior of dielectric films when illuminated with multiple femtosecond laser pulses," Opt. Eng. **44**, 051107 (2005).
16. L. A. Emmert, M. Mero, and W. Rudolph, "Modeling the effect of native and laser-induced states on the dielectric breakdown of wide band gap optical materials by multiple subpicosecond laser pulses," J. Appl. Phys. **108**, 043523 (2010).
17. M. Mende, S. Gunster, H. Ehlers, and D. Ristau, "Optical Properties of Ion Beam Sputtered Oxide Mixture Coatings," *Optical Interference Coatings*, OSA Technical Digest (Optical Society of America, 2010), paper ThA4.
18. M. J. Webber, *Handbook of Optical Materials* (CRC Press, 2003).
19. N. M. Ravindra, P. Ganapathy, and J. Choi, "Energy gap refractive index relations in semiconductors: an overview," Infrared Phys. Technol. **50**, 21–29 (2007).
20. T. S. Moss, "A relationship between the refractive index and the infra-red threshold of sensitivity for photoconductors," Proc. Phys. Soc. London Sect. B **63**, 167 (1950).
21. P. J. L. Herve and L. K. J. Vandamme, "General relation between refractive index and energy gap in semiconductors," Infrared Phys. Technol. **35**, 609–615 (1994).
22. ISO 21254:2011, "Test methods for laser-induced damage threshold," International Organization for Standardization.
23. M. Lenzner, J. Kruger, S. Sartania, Z. Cheng, C. Spielmann, G. Mourou, W. Kautek, and F. Krausz, "Femtosecond optical breakdown in dielectrics," Phys. Rev. Lett. **80**, 4076–4079 (1998).
24. W. Kautek, J. Kruger, M. Lenzner, S. Sartania, C. Spielmann, and F. Krausz, "Laser ablation of dielectrics with pulse durations between 20 fs and 3 ps," Appl. Phys. Lett. **69**, 3146–3148 (1996).
25. A.-C. Tien, S. Backus, H. Kapteyn, M. Murnane, and G. Mourou, "Short-pulse laser damage in transparent materials as a function of pulse duration," Phys. Rev. Lett. **82**, 3883–3886 (1999).
26. N. Sanner, O. Utéza, B. Chimier, M. Sentis, P. Lassonde, F. Légaré, and J. C. Kieffer, "Toward determinism in surface damaging of dielectrics using few-cycle laser pulses," Appl. Phys. Lett. **96**, 071111 (2010).
27. J. Siegel, D. Puerto, W. Gawelda, G. Bachelier, and J. Solis, "Plasma formation and structural modification below the visible ablation threshold in fused silica upon femtosecond laser irradiation," Appl. Phys. Lett. **91**, 082902 (2007).
28. S. W. Winkler, I. M. Burakov, R. Stoian, N. M. Bulgakova, A. Husakou, A. Mermillod-Blondin, A. Rosenfeld, D. Ahkenasi, and I. V. Hertel, "Transient response of dielectric materials exposed to ultrafast laser radiation," Appl. Phys. A **84**, 413–422 (2006).
29. D. Puerto, J. Siegel, W. Gawelda, M. Galvan-Sosa, L. Ehrentraut, J. Bonse, and J. Solis, "Dynamics of plasma formation, relaxation, and topography modification induced by femtosecond laser pulses in crystalline and amorphous dielectrics," J. Opt. Soc. Am. B **27**, 1065–1076 (2010).
30. I. Jovanovic, C. Brown, B. Wattellier, N. Nielsen, W. Molander, B. Stuart, D. Pennington, and C. P. J. Barty, "Precision

short-pulse damage test station utilizing optical parametric chirped-pulse amplification," Rev. Sci. Instrum. **75**, 5193–5202 (2004).
31. B. Chimier, O. Utéza, N. Sanner, M. Sentis, T. Itina, P. Lassonde, F. Légaré, F. Vidal, and J. C. Kieffer, "Damage and ablation thresholds of fused-silica in femtosecond regime," Phys. Rev. B **84**, 094104 (2011).
32. M. Kimmel, P. Rambo, R. Broyles, M. Geissel, J. Schwarz, J. Bellum, and B. Atherton, "Optical damage testing at the Z-backlighter facility at Sandia National Laboratories," Proc. SPIE **7504**, 75041G (2009).
33. N. Sanner, O. Utéza, B. Bussiere, G. Coustillier, A. Leray, T. Itina, and M. Sentis, "Measurement of femtosecond laser-induced damage and ablation thresholds in dielectrics," Appl. Phys. A **94**, 889–897 (2008).
34. D. Du, X. Liu, G. Korn, J. Squire, and G. Mourou, "Laser-induced breakdown by impact ionization in SiO_2 with pulse widths from 7 ns to 150 fs," Appl. Phys. Lett. **64**, 3071–3074 (1994).
35. H. Varel, D. Ashkenasi, A. Rosenfeld, R. Herrmann, F. Noack, and E. E. B. Campbell, "Laser-induced damage in SiO_2 and CaF_2 with picosecond and femtosecond laser pulses," Appl. Phys. A **62**, 293–294 (1996).
36. T. A. Jia, H. X. Chen, M. Huang, F. L. Zhao, X. X. Li, S. Z. Xu, H. Y. Sun, D. H. Feng, C. B. Li, X. F. Wang, R. X. Li, Z. Z. Xu, X. K. He, and H. Kuroda, "Ultraviolet-infrared femtosecond laser-induced damage in fused silica and CaF_2 crystals," Phys. Rev. B **73**, 054105 (2006).
37. The small differences (in the error bars) between the constants published in Ref. [8] and the present paper are due to the fact that more data than published in Ref. [7] are taken into account for the fit.
38. L. Gallais, J. Capoulade, J.-Y. Natoli, M. Commandré, M. Cathelinaud, C. Koc, and M. Lequime, "Laser damage resistance of hafnia thin films deposited by electron beam deposition, reactive low voltage ion plating, and dual ion beam sputtering," Appl. Opt. **47**, C107–C113 (2008).
39. O. Stenzel, S. Wilbrandt, M. Schurmann, N. Kaiser, H. Ehlers, M. Mende, D. Ristau, S. Bruns, M. Vergohl, M. Stolze, M. Held, H. Niederwald, T. Koch, W. Riggers, P. Burdack, G. Mark, R. Schafer, S. Mewes, M. Bischoff, M. Arntzen, F. Eisenkramer, M. Lappschies, S. Jakobs, S. Koch, B. Baumgarten, and A. Tunnermann, "Mixed oxide coatings for optics," Appl. Opt. **50**, C69–C74 (2011).
40. B. J. Pond, J. I. DeBar, C. K. Carniglia, and T. Raj, "Stress reduction in ion beam sputtered mixed oxide films," Appl. Opt. **28**, 2800–2805 (1989).
41. J.-S. Chen, S. Chao, J.-S. Kao, H. Niu, and C.-H. Chen, "Mixed films of TiO_2–SiO_2 deposited by double electron-beam coevaporation," Appl. Opt. **35**, 90–96 (1996).
42. N. K. Sahoo, S. Thakur, and R. B. Tokas, "Achieving superior band gap, refractive index and morphology in composite oxide thin film systems violating the Moss rule," J. Phys. D **39**, 2571–2579 (2006).
43. C.-C. Lee, C.-J. Tang, and J.-Y. Wu, "Rugate filter made with composite thin films by ion-beam sputtering," Appl. Opt. **45**, 1333–1337 (2006).
44. D. Nguyen, L. A. Emmert, I. V. Cravetchi, M. Mero, W. Rudolph, M. Jupe, M. Lappschies, K. Starke, and D. Ristau, "$Ti_xSi_{1x}O_2$ optical coatings with tunable index and their response to intense subpicosecond laser pulse irradiation," Appl. Phys. Lett. **93**, 261903 (2008).
45. N. Bloembergen, "Laser-induced electric breakdown in solids," IEEE J. Quantum Electron. **10**, 375–386 (1974).